manuscripta geodaetica (1988) 13:172–179

manuscripta geodaetica

On carrier signal multipath effects in relative GPS positioning

Y. Georgiadou [1] and A. Kleusberg [2]

[1] Geological Survey of Canada, Geophysics Division, 1 Observatory Cr., Ottawa, Ontario, Canada K1A 0Y3
[2] Geodetic Research Laboratory, University of New Brunswick, Fredericton, N.B., Canada E3B 5A3

Received July 6, 1987; Accepted November 3, 1987

Abstract

We discuss errors in GPS carrier phase observations resulting from multipath interference. A mathematical model for multipath induced carrier phase errors is derived. It is shown that multipath can be monitored over short baselines by analyzing dual frequency measurements. Two related experiments performed by the Geophysics Division of the Geological Survey of Canada are reported. The first example demonstrates that extreme multipath interference can render useless GPS observations for precise positioning applications. The second example shows the danger of occurrence of long periodic multipath errors caused by conducting material in the immediate vicinity of the receiver antenna.

1. Introduction

During the last few years, GPS has proven to be one of the most accurate techniques for the establishment of regional geodetic control. As receiver cost and operation complexity decreases, GPS relative positioning will also be applied to rapid routine surveying. This will include the measurement of many short (0.1 to 2 km) baselines for urban survey control and cadastral purposes. Most likely, the required relative positioning accuracy of 5 to 10 ppm will not be jeopardized by the distance dependent error sources in GPS surveys, such as orbital inaccuracies and unmodelled atmospheric delays. Because of the short baselines involved, distance independent measurement errors originating in the receiving equipment and its immediate environment will contribute the major portion of the total error budget. In contrast to the aforementioned relative positioning for regional geodetic control purposes, the unfavourable error situation for local surveys will deteriorate even more for two reasons:

- long periodic cyclic errors possibly cannot be reduced by averaging during the short observation sessions (e.g. 15 minutes) anticipated and
- observation sites which are selected primarily to fit the necessities of the survey task will not always be in a "clean" non reflective environment.

Multipath errors occur if the received signal is composed of the direct line of sight signal and one or more constituents which have propagated along paths of a different length. Different propagation paths result from either reflection at the transmitting satellite (satellite multipath) or in the surroundings of the receiving antenna (receiver multipath). For the short baselines in local networks, the effect of satellite multipath will be the same at both receiver sites and therefore cancel in differential positioning (Young et al., 1985).

The occurrence of receiver multipath depends primarily on the reflectivity of the antenna environment. If the antenna is kept at the same point, these effects recur after one sidereal day due to repeated satellite-reflector-antenna geometry. Evans (1986) analyzes repeated GPS pseudo range and carrier phase measurements for a number of stations to assign a day to day "pseudo range multipath correlation" coefficient to each station. The effect of multipath on the determination of absolute ionospheric delay from GPS signals is extensively studied by Bishop et al. (1985). This paper also gives estimates on the size of carrier phase multipath errors and concludes that they are barely detectable. Greenspan et al. (1982) deliberately induce carrier phase multipath through a vertical reflector close to the receiving antenna. They confirm the predicted size and time of occurrence of the resulting carrier phase errors through the analysis of adjustment residuals. Tranquilla (1986) and Tranquilla et al. (1986) discuss the sensitivity to multipath of GPS receiving antennas and report results on multipath measurements in controlled environment.

Two other errors originating at the antenna are phase centre variations and antenna imaging. Phase and phase centre variations are due to a non-spherical phase pattern of the antenna; i.e. the measured phase of the same signal is different for varying signal incidence directions. For the type of antenna used in the experiments described in section 3, the effect can be of the order of a few centimetres for differences in the direction of signal incidence of several tens of degrees (Sims, 1985; Kleusberg, 1986a). Obviously, these errors in carrier phase measurements will recur after one sidereal day, provided the orientation of the antenna with respect to the GPS satellites is the same. Antenna phase and phase centre variations are independent of the antenna environment. Antenna imaging results from changes in the

Contribution No 27087 of the Geological Survey of Canada

Offprint requests to: A. Kleusberg

antenna phase pattern induced by conducting material in the immediate vicinity of the antenna (Tranquilla, 1986). Therefore, it can be seen as an environmentally-induced phase centre variation. If the antenna remains at the same site, errors due to imaging problems will repeat after one sidereal day. Although no results for antenna imaging errors have been reported in the GPS related literature, it is expected that their characteristics are comparable to phase centre variations.

The present paper first describes the effect of multipath on GPS carrier phase measurements as a function of the strength of the reflected signal and the satellite-reflector-antenna geometry. The possibility of monitoring multipath with dual frequency GPS receivers is discussed. Two experiments in which multipath was encountered are reported. They are analyzed with regard to the impact of multipath on relative positioning with GPS.

We restrict the discussion of multipath to signal reflections from planar surfaces that are not a part of the antenna itself. Reflections from parts of the antenna, e.g. the antenna ground plane, change the antenna pattern for certain directions of signal incidence independently of the environment and are most conveniently described as antenna phase centre variations. We also do not consider the effect of antenna imaging in this section. However, when analyzing phase observation data in section 3, we will find these two effects are inseparable from multipath errors.

2. Description of carrier signal multipath

This section describes the effect of signal multipath on GPS carrier phase observations. First, the derivations are conceptually limited to the treatment of a single reflector. It is shown that the occurrence of multipath can be detected in dual frequency measurements over short baselines. Finally, the effect of multiple, simultaneous signal reflections is derived. The main goal is to show the order of magnitude of multipath induced carrier phase errors and their relation to the satellite-reflector-antenna geometry.

2.1 Mathematical model

The signal voltage received at the antenna phase centre is a superposition of the direct carrier signal, S_d, and the reflected signal, S_r. The direct signal voltage is described by

$$S_d = V \cos \phi \tag{1}$$

where V denotes the signal voltage amplitude and ϕ is the signal phase. The reflected signal will, in general, have a phase shift, θ, and a reduced signal voltage amplitude, αV, where $0 \le \alpha \le 1$.

$$S_r = \alpha V \cos (\phi + \theta) \tag{2}$$

The received signal contaminated by multipath

$$S = S_d + S_r \tag{3}$$

can be written in the form

$$S = \beta V \cos (\phi + \psi) \tag{4}$$

where the change in signal voltage amplitude is described by

$$\beta = (1 + 2 \alpha \cos \theta + \alpha^2)^{1/2} \tag{5}$$

and

$$\psi = \arctan \{\sin \theta / (\alpha^{-1} + \cos \theta)\} \tag{6}$$

is the carrier phase error due to multipath interference. Assuming $\alpha << 1$ and neglecting squares of α we obtain the simple approximation

$$\psi \approx \alpha \sin \theta. \tag{7}$$

Due to changing geometry between satellite, reflector, and antenna the phase difference θ between direct and reflected signal will slowly vary in time (see below), resulting in cyclic variations of the carrier phase multipath error ψ. For a given α, eqn.(6) yields a maximum phase error (c.f. Bishop et al., 1985)

$$\psi_{max} = \pm \arcsin \alpha \tag{8}$$

for

$$\theta(\psi_{max}) = \pm \arccos (-\alpha). \tag{9}$$

Thus the amplitude of the multipath carrier phase error depends only on the relative signal strength of the reflected signal expressed by the factor α. The maximum possible phase error is obtained for $\alpha = 1$ and amounts to 90 degrees. This phase error equals a range error of about 4.8 cm for phase measurements of the 1.57542 GHz L1 GPS signal.

Eqn.(6) yields for the frequency of the cyclic variations of the carrier phase error

$$f_\psi = (2 \pi)^{-1} \, d\theta/dt. \tag{10}$$

Assuming a planar reflector we obtain geometrically (c.f. Bishop et al., 1985)

$$\theta = (4 \pi h / \lambda) \sin \delta \tag{11}$$

where

- λ is the carrier wavelength
- δ is the satellite elevation above the reflector plane, and
- h is the perpendicular distance of the antenna phase centre from the (not necessarily horizontal) reflector plane.

From eqns. (10) and (11) we obtain for the multipath error frequency

$$f_\psi = (2 h / \lambda) \cos \delta \, d\delta/dt. \tag{12}$$

It can be seen that the following four factors influence the multipath error frequency:

- f_ψ is inversely proportional to the carrier wavelength
- f_ψ is proportional to the perpendicular distance of the antenna phase centre from the reflector
- f_ψ is proportional to the cosine of the elevation δ of the satellite above the reflector plane

- f_ψ is proportional to the rate of change of the elevation of the satellite above the reflector plane.

Depending on the orbital motion of the satellite and the orientation of the reflector plane, the rate of change of the elevation angle may vary according to

$$0 \le |d\delta / dt| \le n r / (r - R) \qquad (13)$$

where n is the mean motion of the satellite, r is the radius of the satellite orbit assumed circular, and R is the radius of the earth. The rotation of the earth has been neglected in eqn. (13). For average values

$$\delta = 45 \text{ degrees}; \; d\delta/dt = n/2 \approx 0.07 \text{ mrad/sec}, \qquad (14)$$

a reflecting plane 30 cm below the antenna phase centre, and measurements of the L1 signal ($\lambda \approx 19$ cm) we obtain from eqn. (12) for the period of the cyclic multipath variations $T_\psi = 107$ min. The same reflector located at $h = 10$ m would produce multipath variations with periods of only 3.2 min. In the extreme case of zero rate of change of δ, the multipath error would contaminate the carrier phase measurements by a constant offset.

2.2 Detection of multipath in dual frequency observations

In GPS carrier phase measurements, the multipath phase error ψ is indistinguishable from a change of the "true" phase of the direct signal. Only the analysis of adjustment residuals could reveal suspicious systematic variations. However, as described in the following section, dual frequency carrier phase observations can be used to detect the occurrence of multipath directly in the measurement records, at least on short baselines.

The main purpose of using both signals, L1 and L2, for geodetic applications of GPS carrier phase measurement is the elimination of the dispersive ionospheric delay. For short baselines the actual differential ionospheric delay will be very small and large variations in the differential ionospheric delay as computed from dual frequency carrier phase measurements will be an indicator of multipath contamination.

As discussed by Bishop et al. (1985), the amplitude of the multipath phase error variations, ψ_{max}, will be identical for two carrier signals of different frequencies; the frequencies of the multipath error variations will be different. For two carrier signals L1 and L2 with wavelengths λ_1 and λ_2, $\lambda_1 < \lambda_2$, we obtain from eqn. (11)

$$\theta_2 = (\lambda_1 / \lambda_2) \; (h_2 / h_1) \; \theta_1 = \kappa \eta \, \theta_1. \qquad (15)$$

For the GPS frequencies, $\kappa = 120 / 154$. In general, the L1 and L2 phase centres of a dual frequency antenna do not coincide and, therefore, $\eta = h_2 / h_1 \neq 1$. The difference Δ (in units of length) between the ionospheric delays experienced by the two carrier signals is given by (e.g. Kleusberg, 1986b)

$$\Delta = \lambda_2 \phi_2 - \lambda_1 \phi_1 + C \qquad (16)$$

where ϕ_1, ϕ_2 are phase observations (in cycles) of the carrier signals L1 and L2 respectively, and the constant C is a linear combination of the carrier phase ambiguities. Eqn. (16) is free of all clock, satellite ephemerides and tropospheric delay errors. Assuming for a moment that the actual ionospheric delay difference is zero, and that the carrier phase measurements are contaminated by multipath, we obtain from eqns. (4), (6), and (16)

$$\begin{aligned} \Delta &= (\lambda_2 \psi_2 - \lambda_1 \psi_1) / 2\pi + C \\ &= \lambda_2 \arctan \{\sin \kappa\eta\theta_1 / (\alpha^{-1} + \cos \kappa\eta\theta_1)\} / 2\pi \\ &\quad - \lambda_1 \arctan \{\sin \theta_1 / (\alpha^{-1} + \cos \theta_1)\} / 2\pi + C \end{aligned} \qquad (17)$$

and eqn. (7) yields the approximation

$$\Delta \approx \alpha / 2\pi \, (\lambda_2 \sin \kappa\eta\theta_1 - \lambda_1 \sin \theta_1) + C. \qquad (18)$$

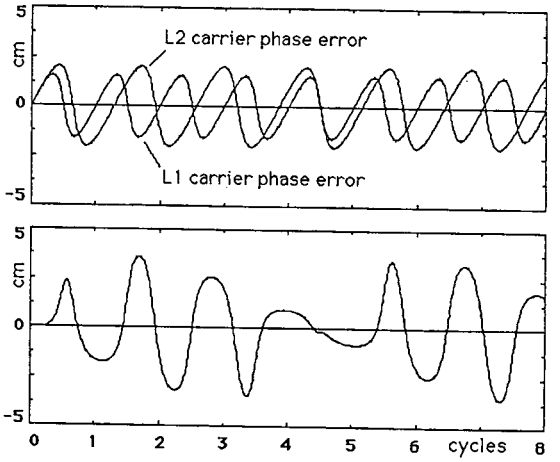

Figure 1: Multipath carrier phase error signatures

Fig. 1 shows theoretical carrier phase error curves due to a reflected signal with voltage amplitude factor $\alpha = 0.5$. The abscissa axis ranges through eight cycles of θ_1. The upper plot is an overlay of single frequency errors for the two GPS carriers, expressed in units of length. The shape of the two curves is similar; but both amplitude and frequency are scaled by the ratio of the carrier wavelengths, κ ($\eta = 1$ has been assumed). The lower plot depicts the resulting "ionospheric delay" errors as computed from eqn. (17) with $C = 0$. The plot is characterized by rather distinct peaks. Whereas the single frequency error curves repeat every cycle of θ_1 or θ_2, the lower curve will repeat only after 77 cycles of θ_1, or 60 cycles of θ_2. According to eqns. (8) and (17), the maximum of the absolute error is $(\lambda_1 + \lambda_2) \arcsin(\alpha)$ which equals 10.7 cm for $\alpha = 1$.

Obviously, the above assumption of zero ionospheric delay in eqn. (17) is not true. However, for short baselines of a few kilometres in length only, the difference between the ionospheric delays experienced by the signals received at the two stations will be very small. Analyzing the differential ionospheric delay

be very small. Analyzing the differential ionospheric delay computed by differencing two eqns. (16) may exhibit structures similar to Fig. 1 and thus may indicate the presence of multipath at either or both observation sites.

2.3 Multiple reflections

The derivations in sections 2.1 and 2.2 were based on the assumption that the multipath is produced by a single reflector. We now consider the case of multiple simultaneous reflections. We denote the i-th reflected signal by

$$S_r^i = \alpha^i V \cos(\phi + \theta^i) \tag{19}$$

and the sum of the direct and all reflected signals by

$$S = S_d + \Sigma_i S_r^i = S_d + V \Sigma_i \alpha^i \cos(\phi + \theta^i). \tag{20}$$

The summation indicated by Σ_i is to be extended over all reflected signals. Using elementary operations, we can rewrite eqn. (20) according to

$$S = \beta V \cos(\phi + \psi) \tag{21}$$

where the total signal voltage amplitude and the multipath induced carrier phase error are given by

$$\beta = \{(1 + \Sigma_i \alpha^i \cos\theta^i)^2 + (\Sigma_i \alpha^i \sin\theta^i)^2\}^{1/2} \tag{22}$$

$$\psi = \arctan\{(\Sigma_i \alpha^i \sin\theta^i) / (1 + \Sigma_i \alpha^i \cos\theta^i)\}. \tag{23}$$

Assuming $\alpha^i << 1$ and neglecting squares and products of α^i, we obtain the approximations

$$\psi \approx \Sigma_i \alpha^i \sin\theta^i \tag{24}$$

and

$$\Delta \approx \Sigma_i \alpha^i (\lambda_2 \sin\kappa\eta^i\theta^i - \lambda_1 \sin\theta^i) / 2\pi + C \tag{25}$$

to replace the single reflector eqns. (7) and (18).

Obviously, the simple structure of the multipath carrier phase error as described in section 2.1 and shown in Fig. 1 is now lost. The strength of the reflected signals will, in general, vary in time and distort the error pattern even more, and a non-planar reflector will lead to different error frequencies. However, reflected signals with dominant amplitude and/or frequency will often prevail in eqns. (23) through (25) and thus enable multipath detection as described in section 2.2.

3. Experimental results

Two experiments were performed to investigate the impact of carrier signal multipath on relative positioning with GPS. To avoid any differential atmospheric delays or errors resulting from inaccurately known satellite orbits, two very short baselines were selected for the tests. Texas Instruments TI4100 equipment was used in both cases and the receivers were operated with GESAR software. Baseline results were computed from the carrier phase observations using the DIPOP program package (Vanicek et al., 1985). Both experiments were repeated the following day.

3.1 Measurement of a 3.5 m baseline

In the first experiment, the two antennas were placed 3.5 metres apart in a highly reflective environment on a flat roof top in Ottawa. Dual frequency carrier phase data were collected at one second intervals between 13:20 UT and 13:40 UT on Dec. 14 and 15, 1986. The satellites tracked were PRN 3, 6, 11, and 12. Figure 2 shows the satellite positions during the observation period in terms of azimuth and elevation.

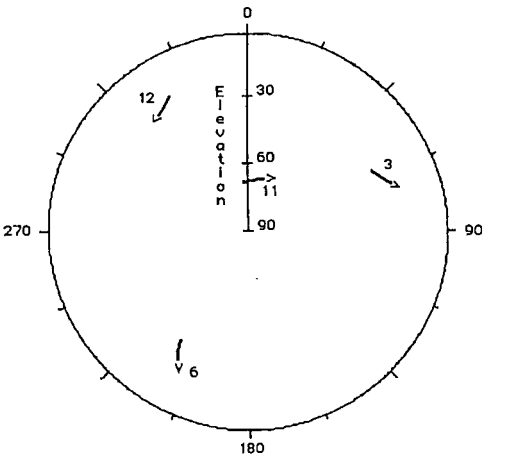

Figure 2: Satellite polar plot, Dec. 14, 1986, 13:30-13:40 UT

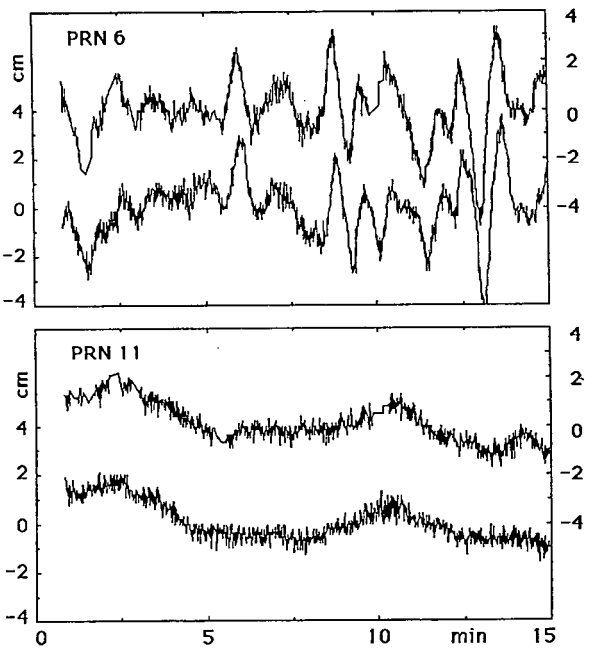

Figure 3: Differential "ionospheric" delay, Dec. 14 - 15, 1986

First, the differential "ionospheric" delay for all satellites was computed according to eqn. (16). The time series so obtained were reduced to a mean value of zero to approximately eliminate the linear combination of ambiguities, C. Figure 3 depicts the resulting variations for satellites 6 and 11 versus elapsed time. Both plots are overlays of the results obtained for Dec. 14 and 15. The upper curves (with labels at the right side of the figure) pertain to Dec. 15. For clarity, they are offset by +2 cm along the vertical axis. Along the time axis, the plots for Dec. 15 are shifted by 236 seconds to allow for direct comparison of delay values obtained for repeated satellite geometry after one sidereal day.

For both satellites, the almost perfect correlation by visual inspection is rather astonishing. The degree of correlation is confirmed in Figure 4. It shows the cross correlation coefficient ρ for the time series in the previous figure as a function of the delay time. The cross correlation for satellite 6 has a peak value of $\rho = 0.84$ for a time delay of 242 seconds. The first side lobes of the correlation function indicate a lower correlation maximum for an additional time delay of $\pm$ 1.5 minutes, resulting from the periodicities of the time series. The peak correlation value for satellite 11 is $\rho = 0.79$ for a time delay of 235 seconds. This correlation function shows no periodicities within the delay window of Figure 4. The high degree of correlation clearly indicates that the variations shown in Figure 3 are related to repeated satellite geometry and, therefore must be attributed to multipath, imaging and phase centre variations. The discrepancies between the theoretical maximum correlation time lag of 236 seconds and the estimated time lags were found to be mainly due to deviations of the satellite orbital periods from their nominal values (Popelar, 1987).

To see the differences between the records for satellite 6 and 11 more clearly, a spectral decomposition was computed for the time series shown in Figure 3. Figure 5 depicts the power spectral density of the "ionospheric" delays observed on Dec. 14. Both curves show a receiver noise power density level of 10-20 mm^2 / Hz for frequencies above 0.05 Hz. If this level is constant throughout the spectrum, it accounts for a rms receiver noise of about 3 mm in the differential ionospheric delay. Assuming uncorrelated errors for both frequencies and receivers, this translates into less then 2 mm rms single frequency single receiver noise (c.f. Evans et al., 1985).

Below 0.05 Hz, both graphs show an increase of power density to about 10^4 mm^2 / Hz for a frequency of 0.002 Hz. But for satellite 6, a major peak up to the same density level is superimposed between 0.007 Hz and 0.025 Hz. It represents the predominant variations in figure 3 with periods between 40 second and 2.5 minutes. According to the model derived in section 2, cyclic variations of these short periods can originate from rather distant (h > 5 m) planar reflectors. However, due to the multitude of conducting material in the surroundings of the observation site, the unambiguous identification of a particular reflector was not possible.

The least squares adjustment of the observations failed to yield reasonable results for the baseline components and the carrier phase double difference ambiguities. The real number ambiguity estimates did not converge to an integer and showed a rather erratic behaviour. The adjustment residuals (see Figure 6), reflected the

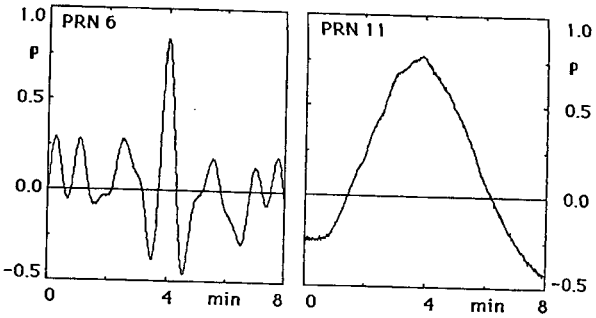

Figure 4: Cross correlation, Dec. 14 and 15, 1986

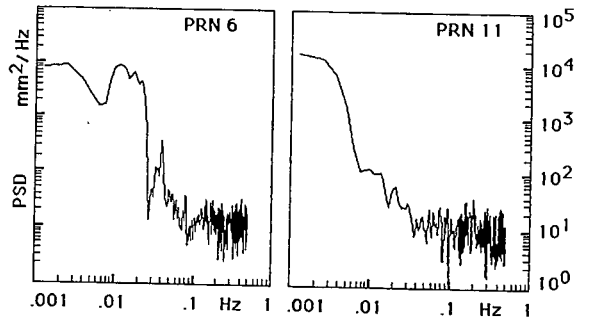

Figure 5: Power Spectral Density of differential "ionospheric" delay

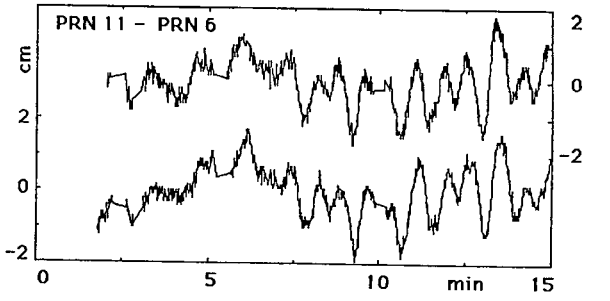

Figure 6: L1 adjustment residuals, Dec. 14 - 15, 1986

short period constituents seen in Figure 3. Since some of the long period variations were absorbed in the parameter estimation, the baseline component results became completely unacceptable. The day to day baseline differences were of the order of several centimetres; differences between L1 and L2 solutions exceeded one decimetre. In short: the relative positioning result was useless.

3.2 Measurement of a 24 m baseline

The second experiment was conducted in the vicinity of Ottawa. One antenna was mounted on a tripod with no conducting material within 15 metres. The other antenna was taped onto a flat aluminum box which was placed on the horizontal corrugated tin roof of a trailer. Carrier phase data was collected at 30 second intervals between 3:20 UT and 5:30 UT on May 7 and 8, 1987. Satellite 6 was tracked between 3:20 UT and 4:20 UT, satellite 11, 12 and 13 throughout the whole session.

Figure 7 shows the positions of the GPS satellites during the observation session in terms of azimuth and elevation. Because of low satellite elevation, the signals of satellites 12 and 13 could be reflected from the corrugated tin roof during the first hour of observations. This type of reflection was also possible for the signal of satellite 6 during the last half hour of tracking. For the remaining observation time, signal reflection was possible only from the flat surface of the above mentioned aluminum box below the antenna.

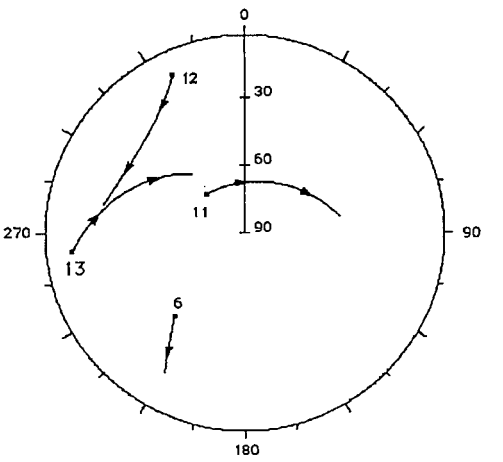

Figure 7: Satellite polar plot, May 7, 1987, 3:20 - 5:30 UT

Figure 8 shows the differential "ionospheric" delay for the May 7 observation session as computed from the carrier phase observations according to eqn. (16). During the aforementioned periods of signal reflection from the roof of the trailer, the variations in the delay curves are rather short periodic and relatively large in amplitude compared to the rest of the observation session. The smooth lines in Figure 8 depict the theoretical multipath effect computed from satellite elevation angles using eqns. (11) and (18). A signal voltage amplitude factor $\alpha = 0.3$ was found to yield the observed error amplitudes. The L1 and L2 phase centres were assumed to coincide with the respective marks on the TI4100 antenna surface giving $h_1 = 24$ cm and $h_2 = 22$ cm. For satellites 6, 11, and 13, the theoretical multipath matches the long periodic variation quite well; the agreement for satellite 12 however is rather disappointing. The differences between theoretical and observed multipath may be due to unmodelled phase centre variations and antenna imaging resulting from the attached aluminum box. The extremely long periods seen in the plots for satellites 11 and 12 deserve special attention. During the 2 hours of observations, these errors can not be reduced significantly by averaging and, most likely, will cause biases in relative positioning results. We recall from section 2.1 that the periods of multipath variations are inverse proportional to the (in the present case very small) height of the antenna phase centre above the reflector. Note that any constant offset between the theoretical and the observed curves in Figure 8 can be due to the approximate removal of the constant C as described in section 3.1.

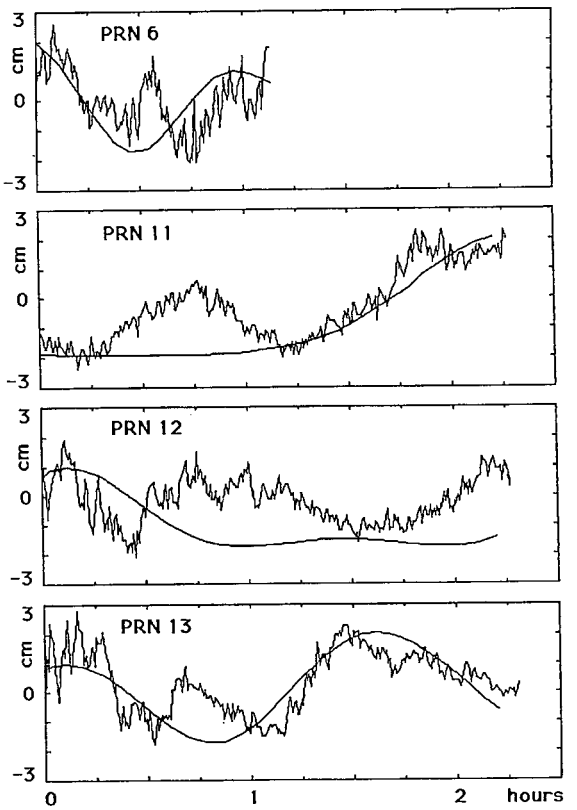

Figure 8: Differential "ionospheric" delay, May 7, 1987

Baseline components were computed for both days from L1 carrier phase observations and the ionospheric delay free linear combination L1/L2 of L1 and L2 measurements. The real number estimates for the carrier phase ambiguities converged to integers and could be held fixed in a subsequent re-processing step. Figure 9 shows the L1 carrier phase double difference adjustment residuals for both days. The residuals for May 8 have been shifted by +2 cm along the vertical axis and by one sidereal day along the time axis to enable a direct comparison of residuals for repeated satellite-antenna geometry. As in the experiment described in section 3.1, the degree of correlation is very high. The cross correlation coefficients of all three residual time series are larger than 0.9 for a time lag of one sidereal day. This again indicates that most of the variations seen in Figure 9 are directly related to repeated geometry.

Figure 10 shows the convergence of the L1 sequential least squares solution with non fixed ambiguities to the final solution obtained with fixed ambiguities represented by a value of zero. The effect of long period multipath errors is obvious: the intermediate solutions for the baseline components oscillate about the final solution and converge to within ± 2 cm only after about 80 minutes. After this time, the estimated real number ambiguities remain within ± 0.2 (cycles) of their integer value and can be fixed to these integers. It can be seen that after 45 minutes of observations the errors in estimated baseline components are still 5 cm and larger.

The day to day repeatability for L1 and L1/L2 solutions was better than 3 mm for all baseline components. But the differences between L1 and L1/L2 solutions of the same day amounted to up to 3 cm. Any difference between L1 and L2 observations is interpreted as being caused by dispersive refraction and used in the L1/L2 solution to correct these refraction effects according to the inverse squared frequency law of dispersion (e.g. Kleusberg, 1986b). Since in the experiments discussed here the difference between L1 and L2 measurements is caused by completely different phenomena, this correction is obviously wrong and leads to biased results.

The aforementioned agreement of better than 3 mm between L1 baseline results for the two days should not be interpreted as a measure for the accuracy of the baseline determination. Comparing the plots related to satellite 11 in Figures 8 and 9 we see that very long period variations caused by multipath have been absorbed in the adjustment process by the baseline components and do not appear anymore in the residuals. Therefore, the L1 solution is biased too, with equal bias for both days.

4. Conclusions

It has been shown in section 2 that signal multipath causes cyclic carrier phase errors much larger than the receiver noise level. The error amplitude depends on the strength of the interfering reflected signal. For a given satellite - receiver geometry, the error frequencies are proportional to the perpendicular distance of the antenna from the reflector plane. In two multipath experiments reported in section 3, the error amplitudes were of the order of centimetres and the error periods varied between less than a minute and several hours. For short baselines, the differential ionospheric delay computed from dual frequency carrier phase observations was shown to be a useful tool to indicate the presence of multipath.

Obviously, the best way to handle multipath problems would be to avoid the vicinity of any conducting material when selecting an observation site. If this is not possible because of other constraints, multipath may be the main error source in the determination of short baselines. Probably, the effect of multipath on relative positioning results can be reduced through averaging if the observation session is sufficiently longer than the longest multipath error period. But this certainly would increase the cost and time consumption of GPS observations beyond the acceptable level for routine surveying applications. The effect of carrier signal multipath may be especially dangerous in kinematic relative GPS positioning since error reduction through averaging in not possible anymore.

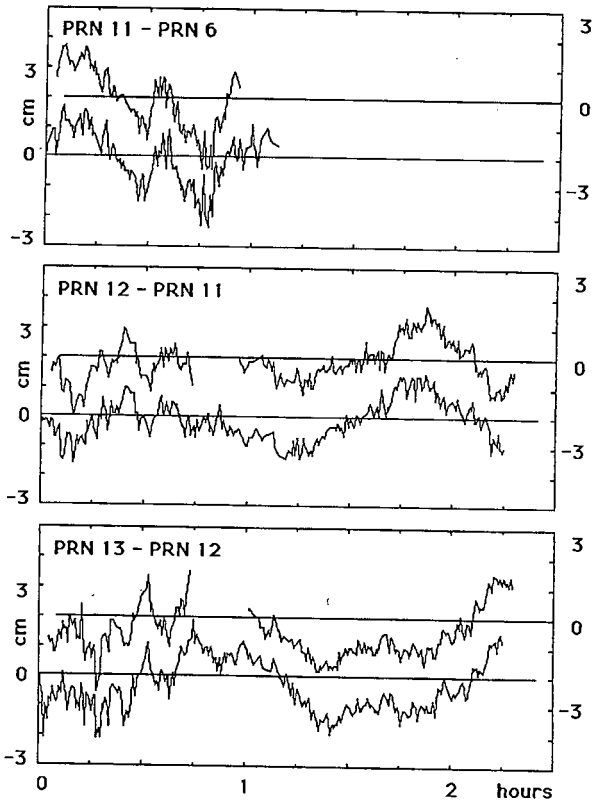

Figure 9: L1 adjustment residuals, May 7 - 8, 1987

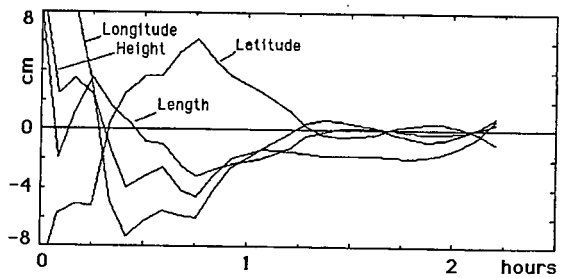

Figure 10: Convergence of L1 solution, May 7, 1987

It should be kept in mind that these conclusions are based on experimental results obtained with a particular type of GPS equipment. Other types of antennas may be less susceptible to multipath interference.

5. Acknowledgements

Assistance from and discussions with A. Goodacre, J. Kouba, R.B. Langley, J. Orosz, J. Popelar, J. Tranquilla and D.E. Wells are appreciated. The research was partially funded through a Natural Sciences and Engineering Research Council (NSERC) visiting fellowship (YG) and NSERC operating grants (AK). This support is gratefully acknowledged.

References

Bishop GJ, Klobuchar JA and Doherty PH (1985): *Multipath effects on the determination of absolute ionospheric delay from GPS signals.* Radio Science 20(3), 388-396

Evans AG (1986): *Comparison of GPS pseudo range and biased Doppler range measurements to demonstrate signal multipath effects.* Proc.4th Intern.Symp.Sat.Pos., Austin,Tx, 28 April - 2 May, 573-587

Evans AG, Herman BR, Coco DS and Clynch JR (1985): *Collocation tests of an advanced Global Positioning System receiver.* Proc.Symp.Pos.GPS, Rockville, MD, April 15-19, 245-254

Greenspan RL, Ng AY, Przyjemski JM and Veale JD (1982): *Accuracy of relative positioning by interferometry with reconstructed carrier GPS: experimental results.* Proc.3rd. Intern.Symp.Sat. Doppler Pos., Las Cruces, NM, Feb.8-12, 1177-1195

Kleusberg A (1986a): *GPS antenna phase centre variations.* EOS Transactions, American Geophysical Union 67 (44) p.911

Kleusberg A (1986b): *Ionospheric propagation effects in geodetic relative GPS positioning.* Manuscripta Geodaetica 11, 256-261

Popelar J (1987): Personal communication

Sims ML (1985): *Phase centre variation in the Geodetic TI4100 GPS receiver system's conical spiral antenna.* Proc.Symp.Pos. GPS, Rockville, MD, April 15-19, 227-244

Tranquilla JM (1986): *Multipath and imaging problems in GPS receiver antennas.* Proc.4th Intern.Symp.Sat.Pos., Austin,Tx, 28 April - 2 May, 557-571

Tranquilla JM, Best SR and Colpitts BG (1986): *Selection and application criteria for GPS receiver antennas.* CGU annual meeting, Ottawa, On., May 19-21

Vanicek P, Beutler G, Kleusberg A, Langley RB, Santerre R and Wells DE (1985): *DIPOP: Differential Positioning Program Package for the Global Positioning System.* Technical Report 115, Department of Surveying Engineering, University of New Brunswick, Fredericton

Young LE, Neilan RE and Bletzacker FR (1985): *GPS satellite multipath: an experimental investigation.* Proc.Symp.Pos.GPS, Rockville, MD, April 15-19, 423-432